

Neuron and Network Modeling

GIORGIO A. ASCOLI and
RUGGERO SCORCIONI

INTRODUCTION

DIGITAL MORPHOMETRY OF SINGLE NEURONS

Computer Acquisition

Digital Files

Dendritic Modeling

AXONAL CONNECTIVITY IN THE ELECTRONIC AGE

Semiautomated Vectorization

Derivation of Connectivity

Models of Axonal Navigation

BOTTOM-UP NETWORK MODELING

System-Level Boundaries and Virtual Stereology

Anatomically Realistic Neural Networks

PHYSIOLOGICAL RELEVANCE

Influence of Morphology on Neuronal Electrophysiology

Network Dynamics

Design Principles

CONCLUSIONS AND FUTURE PERSPECTIVES

APPENDIX

Simple Extraction of Morphometric Parameters with L-Measure

A More Complex Example

REFERENCES

Abstract: Computer technology constitutes a formidable asset in the acquisition, manipulation, analysis, and modeling of neuroanatomical data. Single-cell arborizations can be digitally represented as a large number of connected cylinders. In this form, neuronal structure is amenable to three-dimensional (3D) rendering, extensive quantitative characterization, and computational modeling of biophysics,

GIORGIO A. ASCOLI • Krasnow Institute for Advanced Study and Psychology Department, George Mason University, 4400 University Drive, MS2A1 Fairfax, VA 22030-4444
RUGGERO SCORCIONI • Krasnow Institute for Advanced Study, George Mason University, 4400 University Drive, MS2A1 Fairfax, VA 22030-4444

electrophysiology, outgrowth, network connectivity, and dynamics. This chapter describes the state of the art in neuron and network modeling, with particular emphasis on the methods to acquire, analyze, and synthesize neuroanatomical data. Several commercial and freeware systems are available to reconstruct neuronal morphology in digital format, from a variety of preparations, either directly from the microscope or off-line from captured images. The resulting, increasing amount of digital data (and meta-data) can be archived and publicly distributed to maximize scientific impact. This database enables continuing efforts in modeling dendritic branching of neurons throughout the central nervous system, including cortex, cerebellum, and spinal cord. The experimental acquisition of complete axonal projections from single neurons poses additional challenges, which are only recently being overcome. The combination of dendritic and axonal reconstructions (or models), together with the surface and volumetric representation of the surrounding tissue, allows the computational derivation of synaptic connectivity. Taken together, such models constitute a powerful substrate for the implementation of large-scale, anatomically realistic neural networks. These advances can be instrumental for the cross-scale elucidation of the relationship between structure, activity, and function in the brain.

Keywords: algorithm, axon, computer, connectivity, dendrite, reconstruction, simulation

I. INTRODUCTION

The mammalian brain is often referred to as the “most complex object in the universe.” Indeed, the sheer number of cells and their connections must be compounded with their exquisite organization, from the intricacy of dendritic and axonal branching, to the specificity of the interactions among neuronal classes. Facing such mighty complexity, neuroscientists have traditionally reverted to two levels of analysis. At the system level, descriptions are typically qualitative, with interactions among functional components simply tagged as “present” or “absent” (or perhaps “strong” and “weak”). In contrast, quantitative characterization accompanies the reductionist approach to investigate ever more “elementary” components, from individual cells to spines, synaptic densities, single receptors, their subunits, and individual amino acids. Can the rigorous biophysical knowledge of cellular and subcellular processes be synthesized at the network level?

Computer technology constitutes a formidable asset in the acquisition, manipulation, analysis, and modeling of neuroanatomical data. Models have played a fundamental role in most fields of science, including several sub-disciplines within neurobiology. Neuroanatomy has somehow lagged behind, as its cross-scale complexity prevented the intuitive development of abstract theories. This deadlock can be now solved by adopting hardware and software tools to render neuronal and network structures quantitatively accessible to our understanding. This chapter describes the state of the art in neuron and network modeling, with particular emphasis on the methods to acquire, analyze, and synthesize neuroanatomical data in digital format.

II. DIGITAL MORPHOMETRY OF SINGLE NEURONS

A. Computer Acquisition

Typical neuroanatomical experiments result in chemically processed tissue mounted on a microscope slide. The corresponding observable microscope image can only be further manipulated in a limited way. A key step toward the flexible, quantitative, and extensive analysis and modeling of these data consists of their computer acquisition or *digitization*. The resulting digital files represent data in numerical (machine-readable) format.

Among the essential elements of digital neuroanatomy (as of much of neuroscience) are individual neurons. Ramon y Cajal pioneered the use of *camera lucida*, or drawing tube, a system of mirrors mounted between the microscope oculars and the stage, which allows the precise hand-tracing of the specimen. With this method, still in use in many neuroscience laboratories, neuronal structure is captured on paper as a pencil drawing of its two-dimensional (2D) projection.

Dendritic and axonal trees can be described in digital form as a series of interconnected cylinders, each characterized by the three spatial coordinates of the end point, the diameter, and the identity of the cylinder they are attached to in the path to the soma. Several systems, alternative to camera lucida, have been developed to acquire neuronal morphology directly in digital form. The most widely adopted commercial system is MicroBrightField's NeuroLucida (www.microbrightfield.com). The NeuroLucida setup includes a computer–microscope interface, a motorized stage, and a complete software suite (Glaser and Glaser, 1990). Similarly to the camera lucida system, the user sees the computer's monitor overlaid on the microscopic image. However, instead of drawing with a pencil on paper, the user virtually draws the structure of interest with mouse clicks, and the digital file is created in the computer memory in real time. Fine regulation of the focus is logged as depth, yielding precise spatial information in all three dimensions. The adjustable size of the mouse cursor determines the diameter of the structure being traced. In addition, extended structures can be followed continuously, thanks to the joystick-controlled horizontal movement of the stage, virtually paralleled by corresponding moves on the drawing screen. NeuroLucida also allows the reconstruction of arborizations across multiple serial sections (Fig. 19.1A).

An alternative to the online reconstruction of neurons at the microscope is constituted by the semiautomated acquisition of a *stack* of (possibly tiled) digital images, serially ordered by their depth (or focal plane). Digital reconstruction of neuronal morphology can then be carried out off-line. This system allows lengthy reconstructions to be completed with minimal operation of the (usually expensive) microscope, including from perishable preparations such as fluorescence stains for confocal microscopy. In addition, image stacks can be postprocessed, e.g., by contrast optimization, filtering, and deconvolution.

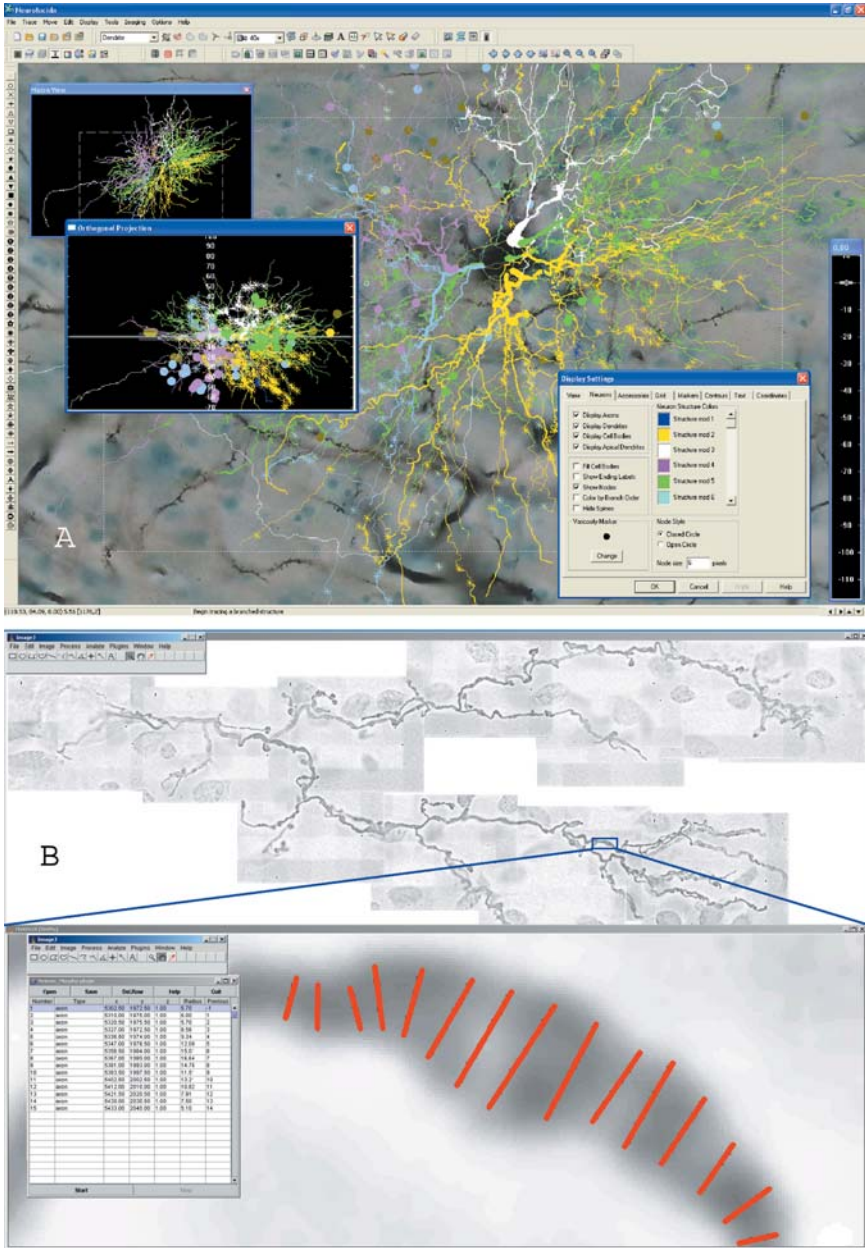


Figure 19.1. Computer-assisted digital reconstructions. (A) Screenshot from MicroBrightField's NeuroLucida[®] software for 3D neuron reconstruction. This image shows neuron reconstruction superimposed on a live image from the microscope. Additional windows provide accessory tools that assist with the neuron tracing are also shown. Neuron reconstruction by Robin Price. (Courtesy of MicroBrightField, Inc.) (B) Neuron_morpho ImageJ plug-in screenshot. The top window contains a cerebellar climbing fiber image from a Z-stack captured by optical microscopy. A portion of this image is enlarged in the bottom window, showing the semimanual tracing operation. Each reconstructed tracing point (red lines) is represented as one row in the inset window. Column entries for each point correspond to a progressive numerical identity, type, x , y , and z coordinates, radius, and identity of the parent segment.

An additional powerful software for the off-line digital reconstruction of neuronal morphology from image stacks is *Neuron_morpho* (Fig. 19.1B), a plug-in of the NIH-distributed imaging program *ImageJ*. Both *ImageJ* (<http://rsb.info.nih.gov/ij>) and *Neuron_morpho* (www.maths.soton.ac.uk/staff/D'Alessandro/morpho) are freely available and run on all JAVA-compatible platforms (including Windows, Linux, and MacOS). Another, less widely used, system for digital reconstruction uses polynomial interpolation to join 2D reconstructions from serial images (Wolf *et al.*, 1995). Several ongoing projects are also attempting to automate the digital reconstruction process by pattern recognition (e.g., He *et al.*, 2003; Rodriguez *et al.*, 2003), an extremely difficult but ultimately commanding step of progress in this field.

B. Digital Files

Digital neuronal morphologies can be displayed and inspected in “pseudo-3D,” including angle views different from that originally imaged under the microscope. *NeuroLucida* offers its own rendering program, called *NeuroExplorer* (Fig. 19.2). An extremely popular neuronal visualization and editing software tool is *Cvapp* (Cannon *et al.*, 1998), a freeware, JAVA-based program that can be run both locally or through a web browser (www.compneuro.org/CDROM/nmorph).

A major advantage of digital representation of neuronal structure is that virtually any geometrical feature captured by the cylinder-based description can be measured and statistically analyzed quickly, reliably, and precisely (see also Appendix). Over 50 morphometric functions can be extracted from single or multiple neuromorphological files with *L-Measure* (Scorcioni and Ascoli, 2001), another JAVA program freely available both for download and web-based usage (Fig. 19.2; www.krasnow.gmu.edu/L-Neuron).

Digital morphologies can be also used to implement anatomically realistic simulations of neuronal biophysics and electrophysiology, e.g., with the popular *NEURON* environment (Hines and Carnevale, 2001; www.neuron.yale.edu). A large collection of such models is available for download and use (Migliore *et al.*, 2003; <http://senselab.med.yale.edu>).

The computer acquisition of digital morphology is considerably labor intensive (~1 week-person per neuron). Thus, researchers willing to share reconstructions with peers provide an invaluable service to the scientific community (Gardner *et al.*, 2003). Several electronic collections of neuronal morphology are available for a variety of cell classes (reviewed in Ascoli, 2002a; Turner *et al.*, 2002). Although almost each archive of neuronal reconstructions comes with its own unique file format (Ascoli *et al.*, 2001a), these can be easily interconverted using tools such as *Cvapp* and *L-Measure*. Nevertheless, particular care must be taken in considering the lab-idiosyncratic morphological characteristics, which can derive from specific experimental conditions and protocols, hardware and software setups, and individual operators' bias (Scorcioni *et al.*, 2004).

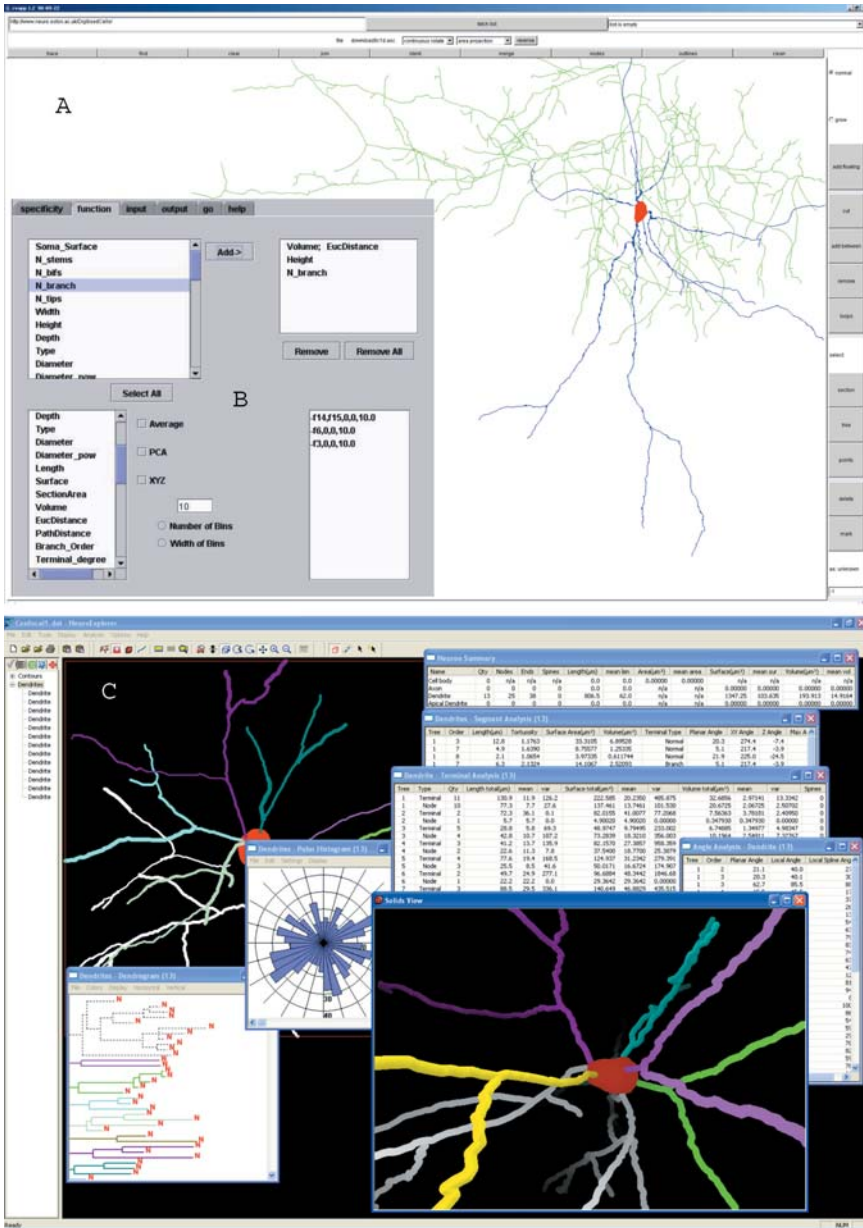


Figure 19.2. Electronic tools for rendering and analyzing neuronal morphology. (A) Cvapp display of a neuron from Markram's neocortical database (<http://microcircuit.epfl.ch>; LBC cell C300301B1 from layer 4). (B) Screenshot (inset) of the L-Measure web-based graphical user interface (see also Appendix). (C) Screenshot from MicroBrightField's NeuroExplorer (TM) software showing results of quantitative morphological analyses and an interactive 3D graphical representation of a reconstructed neuron. (Courtesy of MicroBrightField, Inc.)

C. Dendritic Modeling

A single neuron can be represented in digital form by tens of thousands of 3D coordinates of its branching neurites. This structure can be modeled by designing algorithms to generate synthetic neurons in virtual reality (Ascoli, 1999). The natural variability of neuronal anatomy within a given morphological class can be captured by *stochastic* simulations, in which nonidentical virtual cells are generated in different runs of the model (provided that the seed of random number generation is changed). If the parameters of the algorithm have a straightforward geometric meaning, their statistical distributions can be extracted directly from the populations of real neurons to be modeled (Ascoli and Krichmar, 2000).

A seminal example of this approach is Burke's diameter-based model of dendrogram geometry (reviewed in Burke and Marks, 2002). In this algorithm, dendrites sequentially elongate by a unitary length step, each time sampling diameter dependent, experimentally derived, bifurcation and termination probabilities. If a bifurcation is sampled, two daughter segments are attached at the next steps. If a termination is sampled, the growth of the given branch stops. If neither a bifurcation nor a termination is sampled, another dendritic segment is attached and the process repeats. Originally developed to describe spinal motoneurons, variations of this model have been successfully applied to cerebellar Purkinje cells (Ascoli *et al.*, 2001b) and hippocampal pyramidal cells (Donohue *et al.*, 2002) as well (Fig. 19.3).

Models of dendritic morphology exclusively based on branch diameter are generally under constrained. In other words, the simulated neurons tend to display greater variability than observed in the real cells. In a recent advancement, *hidden variables* (specifically, path distance and the number of terminal tips, or *degree*) were exploited to address this issue. All model parameters were made dependent on the local values of the hidden variables, which were updated at every step of the algorithm. The resulting hidden Markov model successfully captured all relevant properties of dendrogram geometry in hippocampal pyramidal cells (Samsonovich and Ascoli, in press).

An additional element in neuromorphological modeling is the spatial embedding of dendrograms, i.e., the 3D orientation of dendrites. Dendrites can be described as "pointing" in a given absolute direction, or in an orientation relative to the origin of their internal coordinates, i.e., the soma (Ascoli, 1999). A Bayesian method was recently introduced to measure the relative contribution of these various components of tropism from experimental data (Samsonovich and Ascoli, 2003). In all principal cell classes of the rat hippocampus, it was found that the major (and only statistically significant) component of systematic growth was away from the soma. Thus, the heavily polarized shape of hippocampal pyramidal and granule cells may be solely produced by the local orientation of the stems from the soma, which may be genetically determined. As a result, a simple two-parameter model (only specifying the amount of "push" away from the soma, and that of random deflection) can surprisingly capture the emergent shape of these cell classes

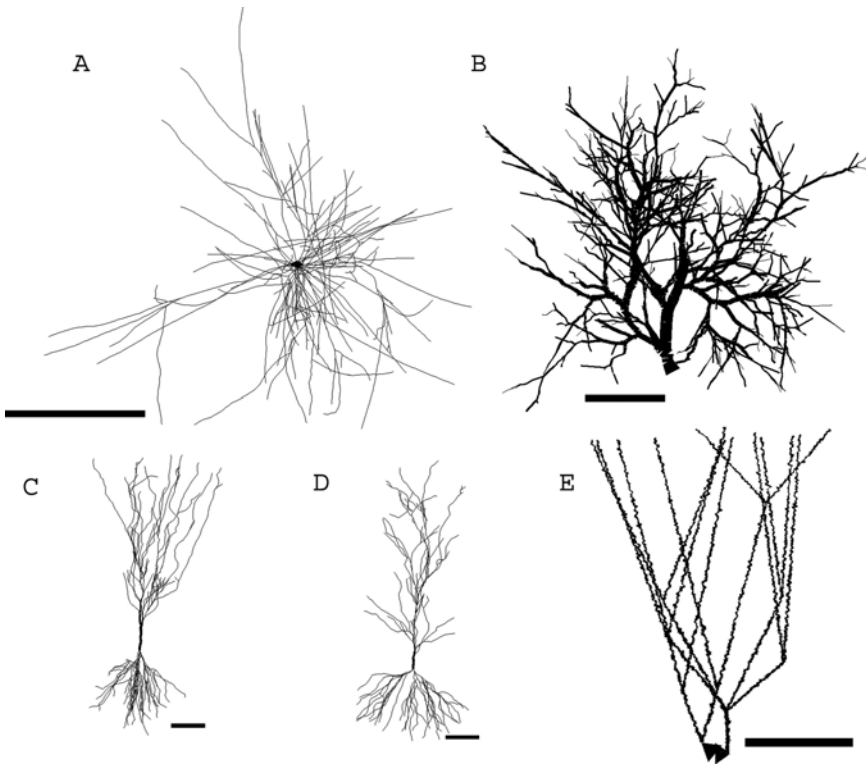


Figure 19.3. Simulated dendritic morphologies. (A) Diameter-based model of a spinal motoneuron. Scale bar: 1000 μm . (B) Diameter-based model of a cerebellar Purkinje cell. Scale bar: 50 μm . (C) Hidden Markov model of a hippocampal CA3 pyramidal neuron. Scale bar: 100 μm . (D) Hidden Markov model of a hippocampal CA1 pyramidal neuron. Scale bar: 100 μm . (E) Globally constrained model of a dentate granule cell. Scale bar: 100 μm .

(Fig. 19.3). Thus, the hidden Markov model of dendrograms and the algorithm of dendritic orientation together constitute a remarkably complete description of neuronal morphology, which was recently also applied to dentate granule cells (Samsonovich and Ascoli, in press).

An alternative model of granule cell morphology was developed based on global constraints such as the position of terminations along the principal component of the dendritic field (Winslow *et al.*, 1999). While the resulting shape coarsely reproduces the structure of real neurons (Fig. 19.3), algorithms of this type cannot be taken (even metaphorically) as *mechanistic* models of development, because real growing branches have access only to locally expressed and stored signals, and not to global information regarding the whole tree or the distal surrounding environment.

Nevertheless, algorithms based on the overall distribution of branching probability against the number of bifurcations, even if a global termination is externally imposed to the whole tree, can still be taken as *descriptive* models

of development, if they capture the temporal dynamics of neuronal growth (Van Ooyen and Van Pelt, 2002). From this point of view, even local models based on dendritic diameter must be considered “hidden,” since the parameter distributions are measured from adult shapes, and kept constant during virtual growth. An extensive review of computational models of neuronal outgrowth, with a discussion of the strengths, weaknesses, and biological plausibility, has been recently published (Donohue and Ascoli, 2004).

III. AXONAL CONNECTIVITY IN THE ELECTRONIC AGE

A. Semiautomated Vectorization

Computer-assisted digital reconstructions of dendritic trees, albeit time-consuming, have now become standard routine in modern cellular neuroanatomy laboratories. The axonal arborizations of projection neurons, however, are simply too huge to be digitized in the same fashion. Only a small number of such reconstructions have been successfully completed in what amounts to a truly heroic effort of dedicated individuals. Camera lucida tracings are still widely adopted to obtain a permanent graphic record of axonal projections from single neurons. How can these data be converted in digital form for improved analysis and modeling?

Pencil drawings can be computer-acquired with a high-resolution scanner, and a segment representation of the tracings can be obtained with freely available software (e.g., www.wintopo.com). Alternatively, camera lucida projections can be directly acquired in electronic form by using computer-interfaced tablets (e.g., Gras and Killman, 1983). In both cases, the result is a set of digitized but disjointed segments (for a technical comparison, see Ewart *et al.*, 1989).

Using a tablet-acquired data set from Tamamaki *et al.* (1988) as a test bed, we have recently developed an algorithm to fully reconnect axonal arborizations in the same format as typically obtained with the techniques described in section “Computer Acquisition” (Fig. 19.4). This implementation (which can be also applied to scanned-in camera lucida paper-and-pencil drawings) simply follows a nearest-neighbor strategy, taking into account the average spread of axonal branches in the thickness of the serial sections (Scorcioni and Ascoli, in press).

Using this semiautomated vectorization procedure, we reconstructed eight complete axonal morphologies from individual neurons, including at least one for each of the principal cell classes of the hippocampal formation: entorhinal cortex layer II stellate cells, dentate gyrus granule cells, CA3, CA2, and CA1 pyramidal cells, and subicular neurons (Fig. 19.5). While the amount of effort required to hand-trace these large arborizations on paper or tablets is still quite considerable, the semiautomated image processing now makes it feasible to obtain larger collections of digital axonal data from each neuronal class.

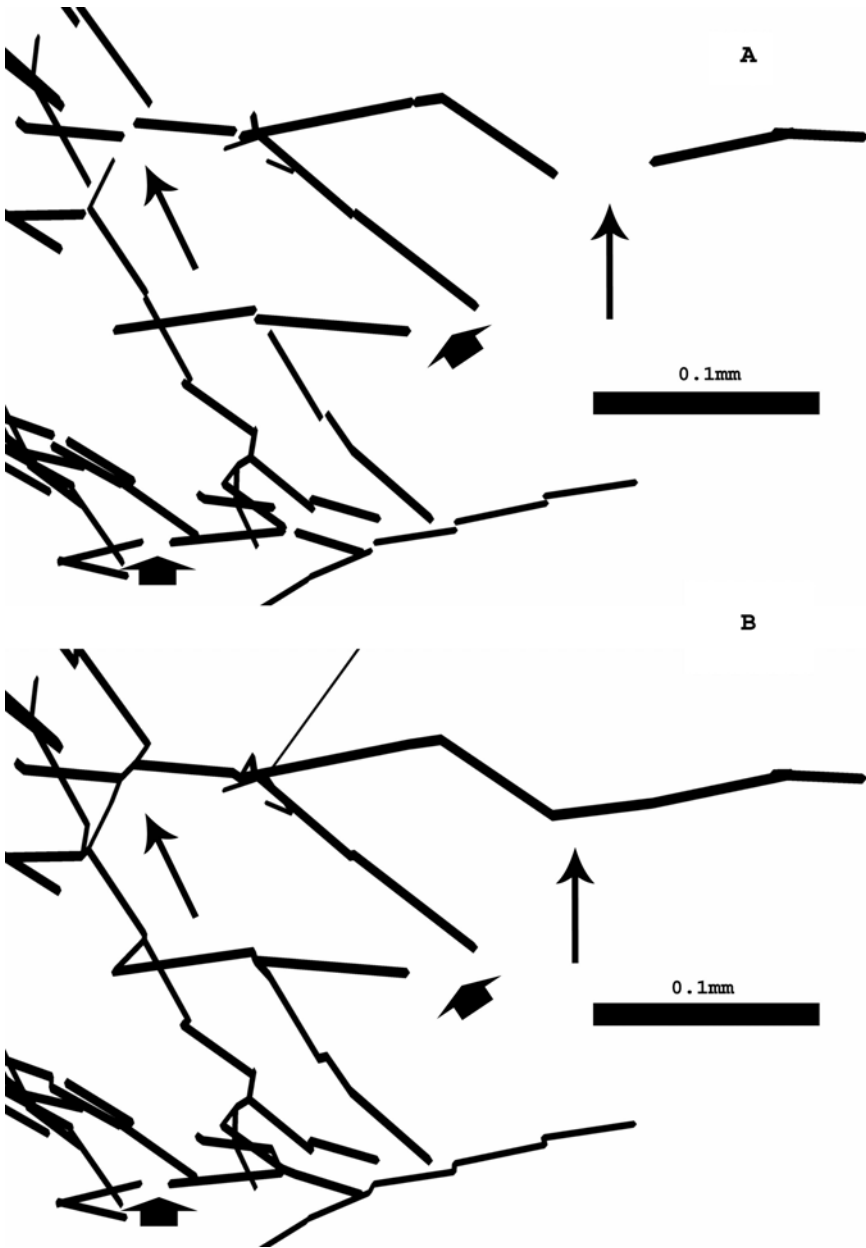


Figure 19.4. Reconstruction of axonal trees from manual tracings. (A) Raw vectorized data. Note various disconnected segments (arrows). (B) Algorithmically connected arborization. Long thin arrows indicate branches that have been joined by an additional segment. Short thick arrows indicate “true” gaps that should remain disconnected in the final reconstruction.

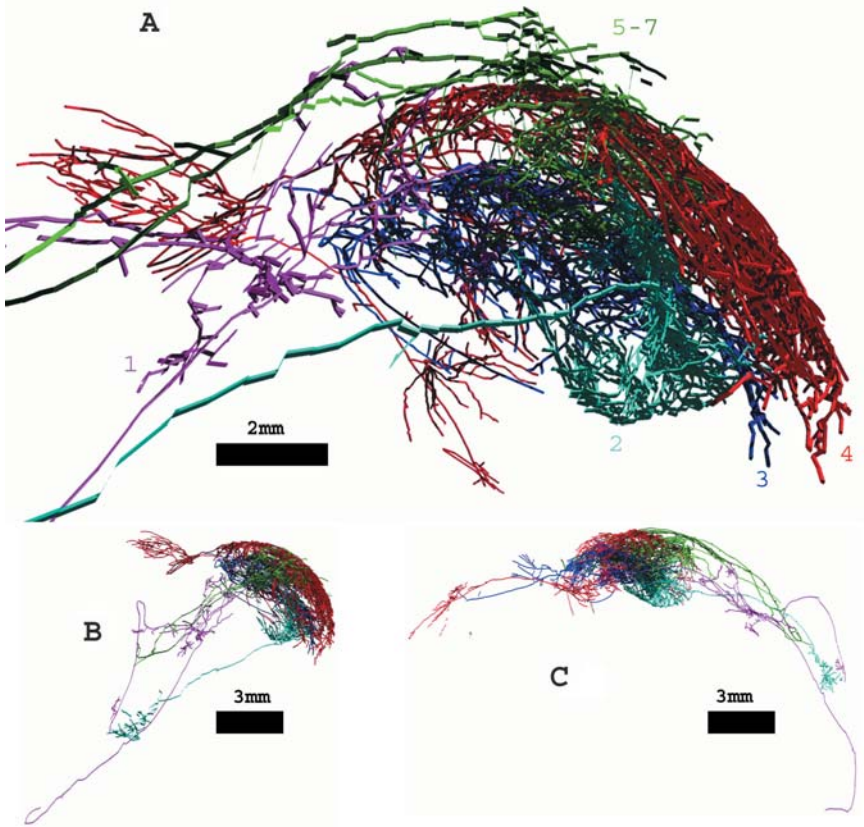


Figure 19.5. Montage of complete ipsilateral projections of one axon from each of the principal cell classes of the hippocampal formation. (A) Lateral view. 1 (purple): subicular pyramidal neuron; 2 (light blue): enthorhinal layer II spiny stellate cell; 3 (dark blue): CA3 pyramidal cell; 4 (red): CA2 pyramidal cell; 5–7 (light-to-dark green): three (distal, medial, and proximal) CA1 pyramidal cells. (B) Horizontal view. (C) Coronal view. (Raw data provided by Dr. N. Tamamaki.)

B. Derivation of Connectivity

A powerful application of digital neuronal reconstructions is constituted by the computational derivation of the potential for connectivity among cell classes. In particular, when axonal and dendritic arborizations share the same anatomical space, it is possible to identify a minimum interaction distance within which synapses could be established. A similar (and computationally equivalent) approach consists of defining a “sphere of influence” around neurites, and analyzing their overlaps. In either case, given an “input” and “output” arborization, it is possible to mathematically derive the number and spatial distribution of potential synapses (e.g., Kalisman *et al.*, 2003).

The relevant geometric parameters for this analysis (e.g., interaction distance) can be estimated from experimental data, such as the size of dendritic spines, the interbouton distance on axons, and the length of growth cones. It is important to stress that this approach yields an estimate of the *potential* for synaptic connectivity, rather than a direct number of synapses. This potential can be regarded as an upper limit of the number of synapses, or as the combinatorial pool of possible synapses, a subset of which is expressed at any given time. In light of the anatomical plasticity of synaptic connections (which are formed and eliminated continuously in at least some regions of the cortex), this measure can be physiologically relevant in the study of the cellular and network bases of learning and memory (Stepanyants *et al.*, 2004).

Potential connectivity is affected both by the intrinsic shape of afferent and efferent cells and by their spatial distribution and orientation. Thus, this type of analysis yields results that are cell-class specific, and can be used to compare different types of neurons within an anatomical region, inferring their possible functional roles (Stepanyants *et al.*, 2004). This approach has also been applied to elucidate the information processing in entire sensory pathways of model systems down to synaptic level (Jacobs and Pittendigh, 2002). Alternatively, it is possible to estimate parameters of the spatial distribution of specific morphologies to ensure effective connectivity of the network (Costa and Manoel, 2003).

Information of system-level connectivity among brain regions is currently being collated in electronic databases, such as the Brain Architecture Management System (Bota and Arbib, 2004; <http://brancusi.usc.edu/bkms>). The advances in computational neuroanatomy described in this and previous sections of this chapter will soon make it possible to create web-based archives of neuronal connectivity at the cellular level (Ascoli and Atkeson, in press).

C. Models of Axonal Navigation

Projecting neurons navigate long distances toward their target before expressing full arborizations in the neuropil (see, e.g., Fig. 19.5). Therefore, computational models of axonal anatomy must include algorithmic descriptions of pathfinding in addition to intrinsic structural determinants. Much is known about the molecular correlates of axonal navigation (e.g., Donohue and Ascoli, 2004). Nonetheless, the theoretical understanding of these complex phenomena is still incomplete, and relatively little information has been so far integrated in computational models.

Senft and Ascoli (1999) proposed a phenomenological model in which axons navigated toward groups of neurons (or glia), turning and possibly bifurcating depending on their local orientation relative to their target, until they arrived within a given distance. At this point, axons started establishing synapses, again turning and bifurcating as necessary to optimally

interact with their local postsynaptic counterparts. After making synaptic contact, the axonal branch in this model was temporarily inhibited from further synapsing. This “refractory period” was a critical parameter of the algorithm, which could discriminate among diverse axonal morphologies such as perforant pathways, sprouting neurites, and climbing fibers (long-, medium-, and short-lasting inhibition, respectively).

Earlier computational models concentrated on a mechanistic description of the biophysical processes underlying axonal movement, such as filopodial dynamics (Buettner, 1995). Several studies have focused on the mathematical description of chemical and cellular gradients as the main guiding cue for axons (e.g., Goodhill, 1998). Increasing attention in computational neuroanatomy is also being paid to the effect of competition (both for external targets and for internal metabolic resources) among axons (Van Ooyen and Van Pelt, 2002). A recent model integrated gradient navigation, axon–axon interaction, and the further influence of patterned activity (Yates *et al.*, 2004). Other relevant efforts include the attempt to describe neuritic navigation and connectivity in 2D with a cell automata formalism (Segev and Ben-Jacob, 2000), and the introduction of cell fate mechanisms in the computational description of axonal pathfinding (Eglen and Willshaw, 2002).

Notably, the relative scarcity of complete axonal reconstructions in digital format prevents a rigorous statistical comparison of the simulated axonal morphologies with the corresponding experimental data. In this sense, a wealth of useful data may become available when the resolution of Diffusion Tensor Imaging reaches the scale of individual axonal bundles (Mori, 2002).

IV. BOTTOM-UP NETWORK MODELING

A. System-Level Boundaries and Virtual Stereology

Axonal projections (and in some cases, dendritic trees as well) are typically affected by system-level geometric constraints, such as the shape of the afferent and efferent nuclei and regions. Thus, in order to fully characterize neuritic shape and neuropil connectivity, it is important to include in the model a digital representation of the relevant tissue and layer boundaries. These data can be acquired from neuroanatomical preparation in ways similar to those described in “Computer Acquisition.” Suitable raw data include high-resolution *ex vivo* microscopic magnetic resonance imaging, or μ -MRI (see, e.g., Lester *et al.*, 2002), cytostructural boundaries traced from intracellular filling experiments (Fig. 19.6), or classic histochemical preparation such as Nissl or myelin stains.

From serially traced system-level boundaries, it is possible to compute continuous surfaces (rendered, e.g., as tiled triangles) and the corresponding volumes (list of internal voxels). Both representations carry important information. Surfaces often determine the orientation of axonal and

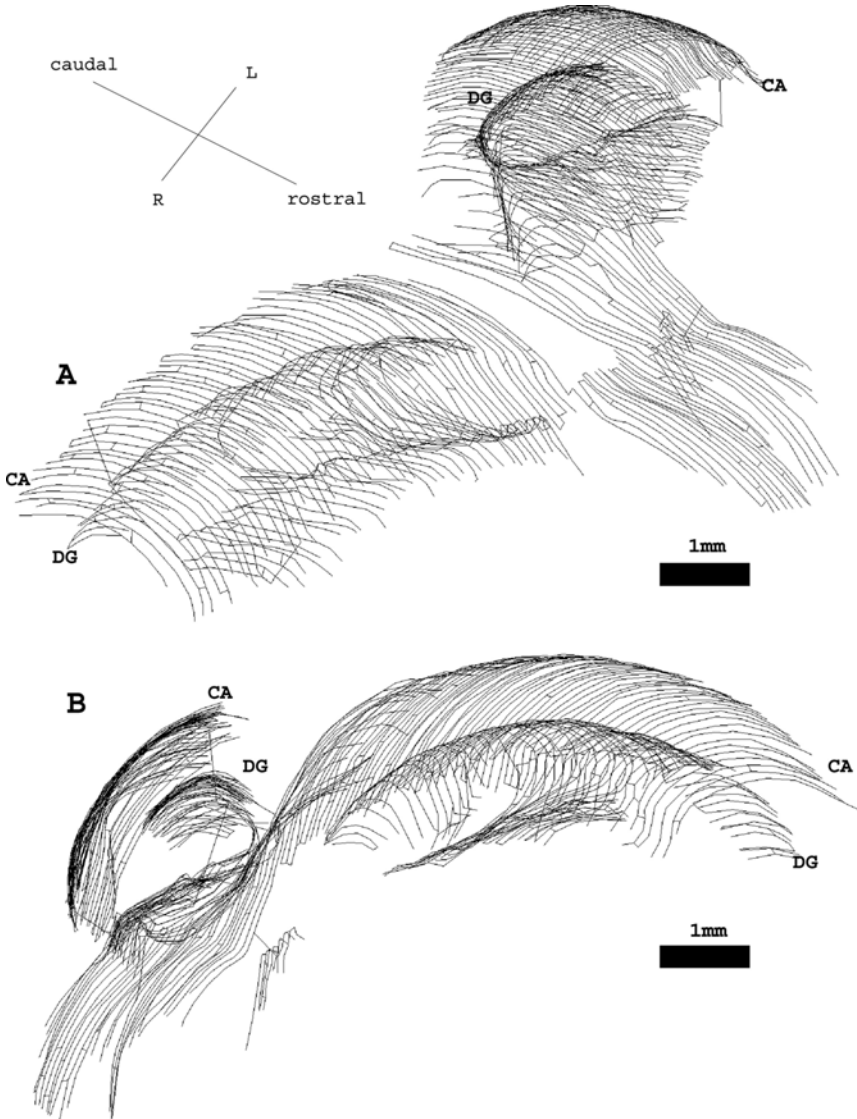


Figure 19.6. Cytostructural boundaries of the rat hippocampus traced from serial sections. (A) Dorsolateral view. Dentate gyrus and Ammon’s horn are clearly visible in both the left and right hippocampi. (B) Mediocaudal view. One of the hippocampi is approximately displayed along its transversal axis, and the other one along its longitudinal axis. (Raw data provided by Dr. N. Tamamaki.)

dendritic arborization, while cell bodies, synapses, and branch coordinates can be virtually positioned in the appropriate volumes. Following this strategy, a large number of reconstructed (or simulated) neurons can be assembled in 3D (Scorcioni *et al.*, 2002) to “recreate” regional anatomy from cellular-level information (Fig. 19.7).

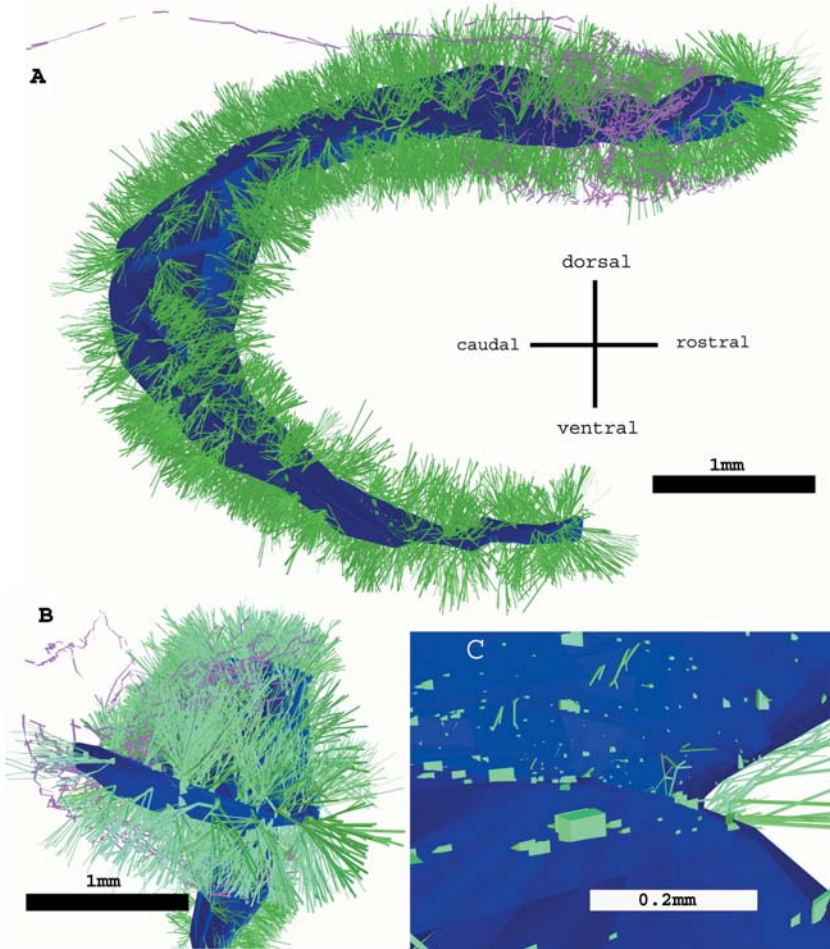


Figure 19.7. Large-scale model of the rat dentate gyrus showing one thousand granule cells (green) over a surface reconstruction of the cellular layer (blue), and the axon from a single spiny stellate cell (purple) projecting from layer II of the entorhinal cortex. (A) Dorsomedial view. (B) Detail on one of the dentate blade endings. (C) Detail from within the hilus. The volume is mostly empty as the granule cell axons (mossy fibers) are not included in the visualization.

Large-scale neuroanatomical models such as those displayed in Fig. 19.7 can be used to compute synaptic connectivity (see section “Derivation of Connectivity”), as well as to impose global constraints to models of neuronal morphology (see “Dendritic Modeling” and “Models of Axonal Navigation”). “Virtual slices” at arbitrary planes of orientation can be explored to foster intuition and guide electrophysiological and anatomical experiments. In addition, basic stereological properties, such as spatial occupancy and density of various subcellular components (e.g., dendrites and axons), can be derived for each layer and position in the

virtual tissue. This approach has been applied to evaluate optimal motoneuron packing in the spinal cord (Burke and Marks, 2002), to quantitatively analyze the basal forebrain corticopetal system (Zaborszky *et al.*, 2002), and the somatosensory cerebro–cerebellar and ascending auditory pathways (Leergaard and Bjaalie, 2002). An important application of this line of study will consist of the inclusion of glia and blood vessels in considering the relationship between structure and function in neural systems.

B. Anatomically Realistic Neural Networks

Biophysical models of single-cell electrophysiology now routinely include a faithful description of neuronal morphology and account for the resulting functional compartmentalization (e.g., Lazarewicz *et al.*, 2002a; Migliore *et al.*, 2003). In contrast, most artificial neural networks have grown increasingly abstract, and retain almost none of the anatomical characteristics of the brain regions they are supposed to represent. Recent efforts, however, have concentrated on the development of anatomically realistic neural network models.

Small networks can be assembled “by hand” out of individual cell models, within the framework of existing modeling environments, such as NEURON (e.g., www.physiol.ucl.ac.uk/research/silver_a/neuroConstruct). Even with massively parallel supercomputers, however, simulation of activity dynamics at the level of subcellular electrophysiological mechanisms can be carried out only for a limited number of neurons. Nevertheless, simple, computationally efficient formalisms exist to capture essential neuronal dynamics (Izhikevich, in press), which can be in principle applied to real-scale network models. The problem remains to automatically and efficiently assemble a realistic anatomical network construct.

The cellular-level anatomy of the CA1 area of a hippocampal slice was simulated with the powerful ArborVitae software (Senft and Ascoli, 1999). Cell bodies for a variety of morphological classes were distributed in layers, subsequently warped to reproduce the natural folds of the rodent archicortex. Dendrites were then virtually grown in 3D using approaches as described in “Dendritic Modeling.” Finally, axons were made to navigate toward and connect with targets specified according to the known wiring diagram of area CA1. The whole simulation could be run, displayed, and saved in a limited amount of time.

Recently, ArborVitae was augmented with the ability to “read in” digital representations of system-level experimental data of layer surfaces and regional volumes. Thus, cells can be distributed according to their precise spatial location, while axons’ navigation can be simulated through a “real” voxel substrate (Senft, 2002). Figure 19.8 shows an example of this application to the simulation of a corticothalamic projection within an imaged human brain.

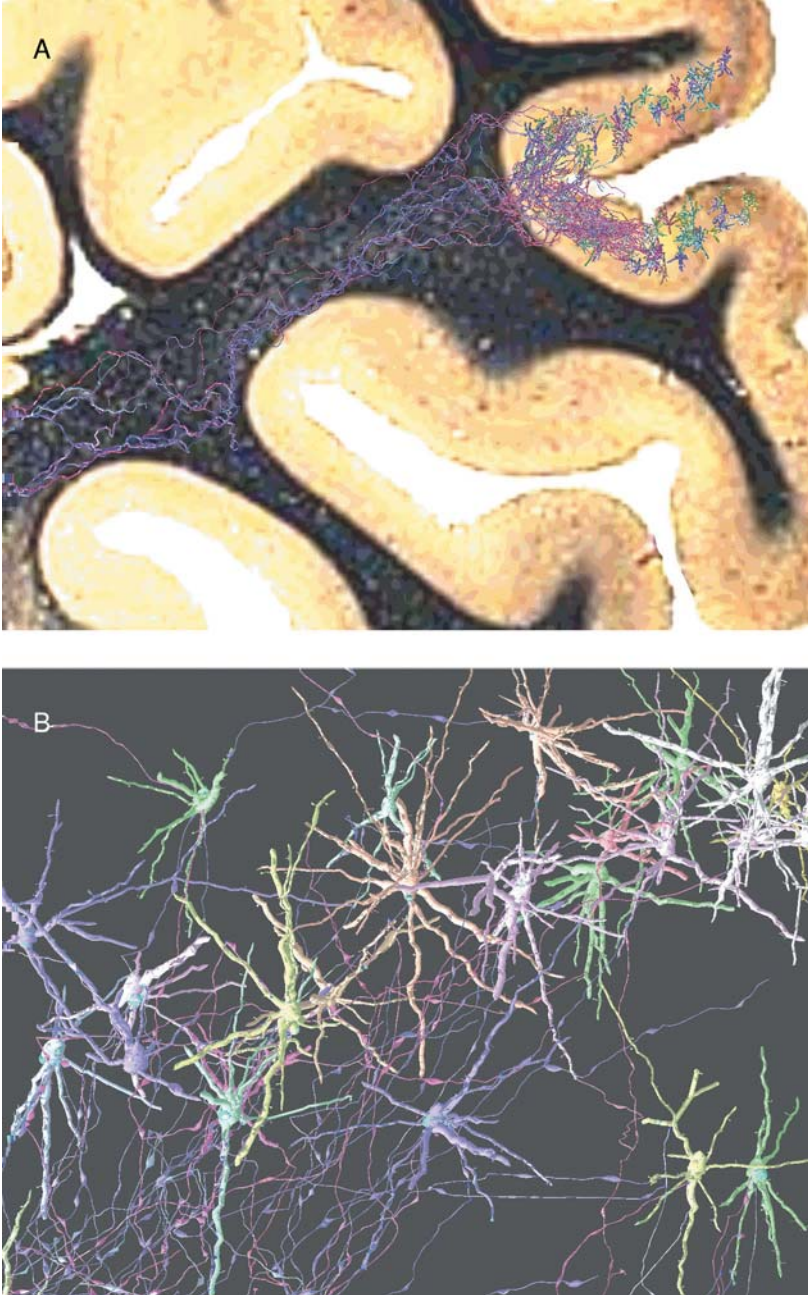


Figure 19.8. An ArborVitae model of human corticothalamic projections. (A) Reverse-contrast display of axons departing from a cortical sulcus and navigating through the white matter toward the thalamus. (B) Zoom-in on the gray matter, with several cortical neurons visible. Unique colors were assigned to each individual cell and its respective processes. (Courtesy of Dr. S. L. Senft.)

The results of ArborVitae simulations can be used to model (offline) the activity dynamics of neuronal populations. The results can then be reloaded for interactive display and analysis. In fact, once the specific connectivity among all cellular classes is obtained from anatomical data (see section “Derivation of Connectivity”), neural network dynamics can be run without the need to explicitly simulate and display the details of network structure (e.g., Ascoli and Atkeson, in press). Three-dimensional arrangements of neurons are however essential to reproduce system-level properties captured by imaging techniques, such as EEG and fMRI, as well as functional interactions with other complex components (e.g., glia).

V. PHYSIOLOGICAL RELEVANCE

A. Influence of Morphology on Neuronal Electrophysiology

Paradoxical as it may sound to the readers of this book, many theoretical neuroscientists question the need to consider anatomy in computational models of the nervous system. In fact, many early computational models of brain function, from the (sub)cellular to the system level, essentially approximated neuroanatomy away. Recent mounting evidence (especially from modeling studies), nevertheless, indicates that both neuronal morphology and network connectivity play a critical role in shaping activity (and thus, presumably, function).

At the cellular level, there is widespread consensus that the integrative properties of dendrites in most neuronal classes are sculpted by their active membrane properties (e.g., Migliore *et al.*, 2003). Voltage-dependent channels, however, are not always uniformly distributed throughout the dendritic trees, creating complex interactions that can only be investigated with numerical simulations. For example, the peculiar bursting activity of CA3 pyramidal cells can be obtained with two distinct channel distributions, but the corresponding subcellular mechanisms are drastically different (Lazarewicz *et al.*, 2002b).

If the distribution of channels is maintained uniform throughout the dendritic trees, nearly all of the known neocortical spiking patterns can simply derive from the different morphologies of the various neuronal classes (Mainen and Sejnowski, 1996). Specifically, the ability of action potentials to forward- and back propagate in the neuronal dendrites of various morphological classes is dramatically variable due to the geometrical difference alone (Vetter *et al.*, 2001). The topological structure of the trees also influences firing patterns (Van Ooyen *et al.*, 2002).

Even the natural variability among individual neurons *within* a morphological class can heavily affect spiking dynamics. When simulated with the same plausible distribution of membrane properties, a set of morphologically accurate CA3 pyramidal cells were shown to fire both regularly and irregularly, with a wide frequency range between 1 and 100 Hz (Krichmar

et al., 2002). Such a morphological control of electrophysiological behavior was robust with respect to the distribution of active channel and the simulation protocols (reviewed in Krichmar and Nasuto, 2002). Similarly, in a combined experimental and computational study, Schaefer *et al.* (2003) showed that temporal integration in neocortical pyramidal cells is affected by the proximal branching pattern in apical trees.

As these biophysical mechanisms relating structure and activity at the single neuron level are uncovered, it is important to critically consider the corresponding subtlety in the representation of digital anatomy in electrophysiological simulations (Lazarewicz *et al.*, 2002a). Depending on both experimental and simulation protocols, morphologies of the same class, reconstructed in different laboratories, can yield more disparate firing properties than can morphologies of different classes, reconstructed in the same laboratory (Scorcioni *et al.*, 2004).

B. Network Dynamics

Since morphology affects the intrinsic excitability of individual neurons, it can be expected to influence network dynamics as well. There are, however, multiple additional avenues of interaction between neuroanatomy and network activity. For example, the spatial location of the neurons and the axonal path length can determine the pattern of onset response latencies (e.g., Kotter *et al.*, 2002).

The typically laminated arrangement of fiber tracts in the cortex also determines the synaptic position in the dendritic layers. This in turn correlates with the electrotonic distance of the input signal from the soma. Even an oversimplified model of passive integration can illustrate that specifying this elementary level of anatomical information deeply changes nearly all dynamical aspects of a recurrent network (Ascoli, 2003). Similar conclusions can be drawn in less orderly and more abstract Hopfield-type networks (Costa *et al.*, 2003).

When multiple cell classes are considered within a subregion, the specific pattern of their connectivity also powerfully modulate the input–output function of neural network (Ascoli and Atkeson, in press). Thus, the function of a given subclass, and the robustness of its contribution to network activity, can be inferred individually for each neuronal class of the subregion. In this perspective, biological neural networks can be viewed as assemblies of functional motifs. The internal anatomy of each motif determines its specific function. Likewise, the anatomy of the motif assembly determines the overall network function.

It should be noted that neuronal structure correlates with and in fact determines all of the above characteristics (time delays, electrotonic distances, synaptic connectivity), as well as the intrinsic firing properties of each morphology class (and individual cell). Thus, the effects of several of these characteristics are likely to be strongly correlated in biological networks. It

is parsimonious to hypothesize that various levels of biophysical organization, such as distribution of dendritic channels, branching pattern, layer position of synapses, and class-specific interconnectivity, coevolved to robustly express the desired network functions. This coevolution may also guarantee a certain degree of homeostatic balance in the resulting activity dynamics.

Given the intricacy of these interactions, computational modeling is extremely useful to separate (at least *in silico*) and quantitatively examine the contributions of each anatomical property to network dynamics. Anatomically realistic neural network models carry the potential to similarly investigate several other mechanisms of interaction between structure and activity. These include, but are not limited to, ephaptic interactions, intrinsic (or extrinsic) electric field modulation of neuronal firing, chemical inhomogeneity in the extracellular medium, glia buffering, and control. Finally, these effects should be expected to be compounded with the natural interindividual variability of neural connectivity, and the related functional and structural effects of (and on) synaptic plasticity.

C. Design Principles

A complementary approach to understanding the physiological relevance of neuron and network anatomy consists of the analysis of the possible principles underlying their structural design. For example, dendritic trees can be observed to increase their space occupancy (i.e., elongate and sprout additional branching) in response to deafferentation, due, e.g., to lesioning of the presynaptic cell population (Shetty and Turner, 1999). This experimental observation could be interpreted by postulating that the principle behind, or goal of (some of the characteristics of), the shape of dendrites is the homeostatic formation of a given number of synapses. This hypothesis can be further tested by altering the number of synapses with a different extrinsic manipulation.

A popular assumption is that biological shape has evolved to *optimize* the expression of its intended function while *minimizing* the metabolic or structural cost, such as the total wiring length of input and output cables (Cherniak *et al.*, 2002). In particular, both the axonal branching pattern (Mitchison, 1992) and the volumetric ratio between axon and dendrites (Chklovskii *et al.*, 2002) appear to be close to optimal in the mammalian neocortex. The clustered organization of cortical connections reflect a key topological characteristic of small-world networks (Hilgetag and Kaiser, *in press*), resulting in highly efficient yield of *functional* connectivity despite a limited *physical* connectivity.

The same design principles can be investigated at larger scales. For example, the spatial placement of macroscopic components of the nervous system (functional subregions in the cortex, or ganglia in invertebrates) can be also compatible with optimal wiring and connectivity (e.g., Young and

Scannell, 1996). Similarly, the intricate spatial pattern of ocular columns may correspond to the optimization of the trade-off between coverage and continuity (Carreira-Perpinan and Goodhill, 2002).

VI. CONCLUSIONS AND FUTURE PERSPECTIVES

A central tenet of neuroinformatics is the digital representation and archiving of (in principle) all relevant information about the nervous system (Ascoli *et al.*, 2003). This goal may constitute a powerful basis for the creation of a large-scale, low-level model of brain structure, activity, and function. Neuroanatomy is leading the pack of success stories in neuroinformatics (Ascoli, 2002b). What is the rationale for envisioning a structural model of the brain, down to the detail of dendritic morphology (Samsonovich and Ascoli, 2002)?

Virtual experiments can be carried out quickly, reliably, safely, and inexpensively. *In silico* investigations can go beyond the boundary of wet lab technical and physical limits (e.g., simultaneously recording from millions of neurons). They allow the exploration of a large number of promising questions, and optimal experimental conditions (only the best of which to be implemented in a “real” experiment). Virtual experiments can also examine the theoretical effect of each model parameter separately by precisely reproducing all other initial conditions. Finally, they limit the use of ethically charged invasive procedures. A detailed, large-scale model of the mammalian brain will also foster scientific education both at the basic and advanced levels.

A simple estimation of the computational power necessary to handle the structure and activity of billions of neurons and trillions of synapses may lead to the conclusion that a truly realistic model of the brain at the cellular level is implausible in any foreseeable future. However, such a model could be dynamically computed piecewise with a multiscale strategy. When virtually recording the overall activity of the cortex, no detail may be necessary about dendritic spines in the cerebellum. Certainly, powerful computational and statistical techniques will be required to exploit such a large-scale model, yet such challenges in *silico* look less insurmountable than those faced when envisioning the corresponding experiments in real brains.

Devil’s advocates will maintain that neuroscience is still too far from the reach of such a grand goal. While this argument is difficult to disagree with, it is relieving to look at the temporal growth of the GeneBank database. From the start of the Human Genome Project (1986), it took 6 years to establish acceptable guidelines, and almost 10 years to complete the yeast genome. Yet only 3 years after that, an entire human chromosome was mapped. It was only one additional year (2000) before all 23 human chromosomes were completed. The clearly exponential graph now looks dramatically flat until the incept of the quite recent boom. The creation of a realistic, large-scale human brain model may follow a similar pattern.

Although the computational power of hardware and software is increasing at an exponential rate, so is the amount of experimental data collected in biomedical sciences in general, and neuroscience in particular. In principle, much of these data need to be incorporated in the realistic model. Neuroinformatics started when experimental neuroscience was already a mature field. Is modeling catching up, or is the gap between relevant published data and corresponding computational simulations ever widening?

The answer to this question depends on what is meant by “relevant,” i.e., what level of modeling computational neuroscientists are designing. This, in turn, is defined by the type of scientific explanation being sought, e.g., behavior in terms of genes, network rhythms in terms of neuronal spiking properties, synaptic strength in terms of calcium buffering. In this perspective, computational models become a constructive definition of our quantitative understanding of the structure, activity, and function of the nervous system. The “ultimate race” between experiments and models, then, is along the fine line dividing data and knowledge.

APPENDIX

A. Simple Extraction of Morphometric Parameters with L-Measure

Common measurements extracted from neuronal morphology include total neuronal length and minimum, average, and maximum dendritic diameter. As a first basic example, a step-by-step guide is given, showing how to extract these basic parameters with L-Measure. Only requirements are an Internet connection and a JAVA-enabled browser.

1. Connect to the online version of L-Measure at www.krasnow.gmu.edu/L-Neuron (click “L-Measure” in the left column, then click “Online Version”). A security window will appear to ask for access permission, click “Yes.”
2. From the panel “Function,” select “Length” in the top left box, and then click “Add.” A new measurement “Length” will appear in the list of functions to be measured on the right.
3. From the same panel, add function “Diameter.”
4. From the panel “Input,” open and add the neurons you wish to analyze and measure. You can freely download electronic neuronal sample from www.krasnow.gmu.edu/L-Neuron (click “Morphology Database”).
5. From the panel “Go” click the “Go” button. L-Measure will list all extracted measurements in the bottom panel. For each selected function, L-Measure displays six values:
 - a. Total sum: In case of “Length” this is the total sum of all segment lengths, which represents the first desired measurement.

- b. Compartments included: It lists how many compartments were included in this measurement.
- c. Compartments excluded.
- d. Minimum value: It reports the minimum value for the specified function. In the diameter row, this represents the second desired measurement.
- e. Average value: It reports the average value across all segments (the third desired measurement).
- f. Maximum value: In the diameter row, this represents the fourth desired measurement.
- g. Standard deviation.

B. A More Complex Example

This section illustrates a more complex example in which a Sholl diagram of length vs. Euclidean distance is generated from basal dendrites with a sphere radial increment of 50 μm . For this section, a pyramidal cell in SWC file format is required, which can be freely downloaded from www.krasnow.gmu.edu/L-Neuron (click “Morphology Database”).

1. Connect to the online version of L-Measure at www.krasnow.gmu.edu/L-Neuron (click “L-Measure” in the left column).
2. From the “Specificity” panel, select the function “Type” and insert the value “3” followed by the “=” radio button. Then click the “Add” button (type = 3 in SWC files identifies basal dendrites).
3. From the top left box in the “Function” panel, select “Length.”
4. From the bottom left box, select “Euclidean Distance.”
5. Select “Width of Bins” from the bottom radio button, and insert a value of 50.
6. Click the “Add” button. A new function named “Length vs. Euclidean Distance” will be added to the right top panel.
- 7-A. In the “Input” panel, add the SWC neuronal reconstruction file.
8. In the “Go” panel, click the “Go” button. The bottom box will show the resulting measurement table.

To obtain a graphical representation of the Sholl diagram, additional steps are required together with a spreadsheet-like software, such as Microsoft Excel. To obtain an Excel compatible output, insert the following extra step into the above sequence:

- 7-B. In the “Output” panel, click the “Save As” button, choose a directory, and write “example.xls.”
9. Double-click the produced “.xls” file. Microsoft Excel will automatically recognize and open the selected file.
10. Within Excel, select the first two rows.

11. Click the “Chart Wizard” button.
12. Select “XY scatterplot.”
13. Press “finish.”

ACKNOWLEDGMENTS. The authors are grateful to Drs. Stephen L. Senft and Nobuaki Tamamaki, and to MicroBrightField, Inc., for supplying material used in some of this chapter’s illustrations. Support was provided by R01 grants NS39600 (jointly funded by NINDS, NIMH, and NSF under the Human Brain Project) and AG025633 as part of the NSF/NIH Collaborative Research in Computational Neuroscience Program.

REFERENCES

- Ascoli, G. A., 1999, Progress and perspectives in computational neuroanatomy, *Anat. Rec.* **257**(6):195–207.
- Ascoli, G. A., 2002a, Neuroanatomical algorithms for dendritic modelling, *Network* **13**(3):247–260.
- Ascoli, G. A., 2002b, Computing the brain and the computing brain, In: Ascoli, G. A. (ed.), *Computational Neuroanatomy: Principles and Methods*, Totowa, NJ: Humana Press, pp. 3–26.
- Ascoli, G. A., 2003, Passive dendritic integration heavily affects spiking dynamics of recurrent networks, *Neural Netw.* **16**:657–663.
- Ascoli, G. A., and Atkeson, J. C., 2005, Incorporating anatomically realistic cellular-level connectivity in neural network models of the rat hippocampus, *Biosystems.* **79**:173–181.
- Ascoli, G. A., De Schutter, E., and Kennedy, D. N., 2003, An information science infrastructure for neuroscience, *Neuroinformatics* **1**(1):1–2.
- Ascoli, G. A., and Krichmar, J. L., 2000, L-Neuron: a modeling tool for the efficient generation and parsimonious description of dendritic morphology, *Neurocomputing* **32–33**:1003–1011.
- Ascoli, G. A., Krichmar, J. L., Nasuto, S. J., and Senft, S. L., 2001a, Generation, description, and storage of dendritic morphology data, *Philos. Trans. R. Soc. Lond. B Biol. Sci.* **356**(1412):1131–1145.
- Ascoli, G. A., Krichmar, J. L., Scorcioni, R., Nasuto, S. J., and Senft, S. L., 2001b, Computer generation and quantitative morphometric analysis of virtual neurons, *Anat. Embryol.* **204**(4):283–301.
- Bota, M., and Arbib, M. A., 2004, Integrating databases and expert systems for the analysis of brain structures: connections, similarities, and homologies, *Neuroinformatics* **2**(1):19–58.
- Buettner, H. M., 1995, Computer simulation of nerve growth cone filopodial dynamics for visualization and analysis, *Cell Motil. Cytoskeleton* **32**(3):187–204.
- Burke, R. E., and Marks, W. B., 2002, Some approaches to quantitative dendritic morphology, In: Ascoli, G. A. (ed.), *Computational Neuroanatomy: Principles and Methods*, Totowa, NJ: Humana Press, pp. 27–48.
- Cannon, R. C., Turner, D. A., Pyapali, G. K., and Wheal, H. V., 1998, An online archive of reconstructed hippocampal neurons, *J. Neurosci. Methods* **84**(1–2):49–54.
- Carreira-Perpinan, M. A., and Goodhill, G. J., 2002, Development of columnar structures in visual cortex, In: Ascoli, G. A. (ed.), *Computational Neuroanatomy: Principles and Methods*, Totowa, NJ: Humana Press, pp. 337–358.
- Cherniak, C., Mokhtarzada, Z., and Nodelman, U., 2002, Optimal-wiring models of neuroanatomy, In: Ascoli, G. A. (ed.), *Computational Neuroanatomy: Principles and Methods*, Totowa, NJ: Humana Press, pp. 71–82.

- Chklovskii, D. B., Schikorski, T., and Stevens, C. F., 2002, Wiring optimization in cortical circuits, *Neuron* **34**(3):341–347.
- Costa Lda, F., and Manoel, E. T., 2003, A percolation approach to neural morphometry and connectivity, *Neuroinformatics* **1**(1):65–80.
- Costa Lda, F., Barbosa, M. S., Coupeuz, V., and Stauffer, D., 2003, Morphological Hopfield networks, *Brain Mind* **4**:91–105.
- Donohue, D. E., and Ascoli, G. A., 2005, Models of neuronal outgrowth, In: Koslow, S. H., and Subramaniam, S. (eds.), *Databasing the Brain: From Data to Knowledge*, Wiley, New York, NY, pp. 303–323.
- Donohue, D. E., Scorcioni, R., and Ascoli, G. A., 2002, Generation and description of neuronal morphology using L-Neuron: a case study, In: Ascoli, G. A. (ed.), *Computational Neuroanatomy: Principles and Methods*, Totowa, NJ: Humana Press, pp. 49–70.
- Eglen, S. J., and Willshaw, D. J., 2002, Influence of cell fate mechanisms upon retinal mosaic formation: a modelling study, *Development* **129**(23):5399–5408.
- Ewart, D. P., Kuzon, W. M., Jr., Fish, J. S., and McKee, N. H., 1989, Nerve fibre morphometry: a comparison of techniques, *J. Neurosci. Methods* **29**(2):143–150.
- Gardner, D., Toga, A. W., Ascoli, G. A., Beatty, J. T., Brinkley, J. F., Dale, A. M., Fox, P. T., Gardner, E. P., George, J. S., Goddard, N., Harris, K. M., Herskovits, E. H., Hines, M. L., Jacobs, G. A., Jacobs, R. E., Jones, E. G., Kennedy, D. N., Kimberg, D. Y., Mazziotta, J. C., Miller, P. L., Mori, S., Mountain, D. C., Reiss, A. L., Rosen, G. D., Rottenberg, D. A., Shepherd, G. M., Smalheiser, N. R., Smith, K. P., Strachan, T., Van Essen, D. C., Williams, R. W., and Wong, S. T., 2003, Towards effective and rewarding data sharing, *Neuroinformatics* **1**(3):289–295.
- Glaser, J. R., and Glaser, E. M., 1990, Neuron imaging with NeuroLucida—a PC-based system for image combining microscopy, *Comput. Med. Imaging Graph.* **14**(5):307–317.
- Goodhill, G. J., 1998, Mathematical guidance for axons, *Trends Neurosci.* **21**(6):226–231.
- Gras, H., and Killmann, F., 1983, NEUREC—a program package for 3D-reconstruction from serial sections using a microcomputer, *Comput. Programs Biomed.* **17**(1–2):145–155.
- He, W., Hamilton, T. A., Cohen, A. R., Holmes, T. J., Pace, C., Szarowski, D. H., Turner, J. N., and Roysam, B., 2003, Automated three-dimensional tracing of neurons in confocal and brightfield images, *Microsc. Microanal.* **9**(4):296–310.
- Hilgetag, C. C., and Kaiser, M., 2004, Clustered organisation of cortical connectivity, *Neuroinformatics* **2**:353–360.
- Hines, M. L., and Carnevale, N. T., 2001, NEURON: a tool for neuroscientists, *Neuroscientist* **7**(2):123–135.
- Izhikevich, E. M., 2004, Which model to use for cortical spiking neurons? *IEEE Trans. Neural Netw.* **15**:1063–1070.
- Jacobs, G. A., and Pittendrigh, C. S., 2002, Predicting emergent properties of neuronal ensembles using a database of individual neurons, In: Ascoli, G. A. (ed.), *Computational Neuroanatomy: Principles and Methods*, Totowa, NJ: Humana Press, pp. 151–170.
- Kalisman, N., Silberberg, G., and Markram, H., 2003, Deriving physical connectivity from neuronal morphology, *Biol. Cybern.* **88**(3):210–218.
- Kotter, R., Nielsen, P., Dyhrfeld-Johnsen, J., Sommer, F. T., and Northoff, G., 2002, Multi-level neuron and network modeling in computational neuroanatomy, In: Ascoli, G. A. (ed.), *Computational Neuroanatomy: Principles and Methods*, Totowa, NJ: Humana Press, 359–382.
- Krichmar, J. L., and Nasuto, S. J., 2002, The relationship between neuronal shape and neuronal activity, In: Ascoli, G. A. (ed.), *Computational Neuroanatomy: Principles and Methods*, Totowa, NJ: Humana Press, pp. 105–126.
- Krichmar, J. L., Nasuto, S. J., Scorcioni, R., Washington, S. D., and Ascoli, G. A., 2002, Effects of dendritic morphology on CA3 pyramidal cell electrophysiology: a simulation study, *Brain Res.* **941**(1–2):11–28.
- Lazarewicz, M. T., Boer-Iwema, S., and Ascoli, G. A., 2002a, Practical aspects in anatomically accurate simulations of neuronal electrophysiology, In: Ascoli, G. A. (ed.), *Computational Neuroanatomy: Principles and Methods*, Totowa, NJ: Humana Press, pp. 127–148.
- Lazarewicz, M. T., Migliore, M., and Ascoli, G. A., 2002b, A new bursting model of CA3 pyramidal cell physiology suggests multiple locations for spike initiation, *Biosystems* **67**:129–137.

- Leergaard, T. B., and Bjaalie, J. G., 2002, Architecture of sensory map transformations: axonal tracing in combination with 3-d reconstruction, geometric modeling, and quantitative analyses, In: Ascoli, G. A. (ed.), *Computational Neuroanatomy: Principles and Methods*, Totowa, NJ: Humana Press, pp. 199–218.
- Lester, D. S., Hanig, J. P., and Pine, P. S., 2002, Quantitative neurotoxicity, In: Ascoli, G. A. (ed.), *Computational Neuroanatomy: Principles and Methods*, Totowa, NJ: Humana Press, pp. 383–400.
- Mainen, Z. F., and Sejnowski, T. J., 1996, Influence of dendritic structure on firing pattern in model neocortical neurons, *Nature* **382**(6589):363–366.
- Migliore, M., Morse, T. M., Davison, A. P., Marenco, L., Shepherd, G. M., and Hines, M. L., 2003, ModelDB: making models publicly accessible to support computational neuroscience, *Neuroinformatics* **1**(1):135–139.
- Mitchison, G., 1992, Axonal trees and cortical architecture, *Trends Neurosci.* **15**(4):122–126.
- Mori, S., 2002, Principle and applications of diffusion tensor imaging: a new MRI technique for neuroanatomical studies, In: Ascoli, G. A. (ed.), *Computational Neuroanatomy: Principles and Methods*, Totowa, NJ: Humana Press, pp. 271–292.
- Rodriguez, A., Ehlenberger, D., Kelliher, K., Einstein, M., Henderson, S. C., Morrison, J. H., Hof, P. R., and Wearne, S. L., 2003, Automated reconstruction of three-dimensional neuronal morphology from laser scanning microscopy images, *Methods* **30**(1):94–105.
- Samsonovich, A. V., and Ascoli, G. A., 2002, Towards virtual brains, In: Ascoli, G. A. (ed.), *Computational Neuroanatomy: Principles and Methods*, Totowa, NJ: Humana Press, pp. 425–436.
- Samsonovich, A. V., and Ascoli, G. A., 2003, Statistical morphological analysis of hippocampal principal neurons indicates cell-specific repulsion of dendrites from their own cell, *J. Neurosci. Res.* **71**(2):173–187.
- Samsonovich, A. V., and Ascoli, G. A., 2005, Statistical determinants of dendritic morphology in hippocampal pyramidal neurons: a hidden Markov model, *Hippocampus* **15**: 166–183.
- Samsonovich, A. V., and Ascoli, G. A., 2005, Algorithmic description of hippocampal granule cell dendritic morphology, *Neurocomputing* **65–66**:253–260.
- Schaefer, A. T., Larkum, M. E., Sakmann, B., and Roth, A., 2003, Coincidence detection in pyramidal neurons is tuned by their dendritic branching pattern, *J. Neurophysiol.* **89**(6):3143–3154.
- Scorcioni, R., and Ascoli, G. A., 2001, Algorithmic extraction of morphological statistics from electronic archives of neuroanatomy, *Lect. Notes Comp. Sci.* **2084**:30–37.
- Scorcioni, R., and Ascoli, G. A., 2005, Algorithmic reconstruction of complete axonal arborizations in rat hippocampal neurons, *Neurocomputing* **65–66**:15–22.
- Scorcioni, R., Boutiller, J. M., and Ascoli, G. A., 2002, A real scale model of the dentate gyrus based on single-cell reconstructions and 3D rendering of a brain atlas, *Neurocomputing* **44–46**:629–634.
- Scorcioni, R., Lazarewicz, M. T., and Ascoli, G. A., 2004, Quantitative morphometry of hippocampal pyramidal cells: differences between anatomical classes and reconstructing laboratories, *J. Comp. Neurol.* **473**(2):177–193.
- Segev, R., and Ben-Jacob, E., 2000, Generic modeling of chemotactic based self-wiring of neural networks, *Neural Netw.* **13**(2):185–199.
- Senft, S. L., 2002, Axonal navigation through voxel substrates: a strategy for reconstructing brain circuitry, In: Ascoli, G. A. (ed.), *Computational Neuroanatomy: Principles and Methods*, Totowa, NJ: Humana Press, pp. 245–270.
- Senft, S. L., and Ascoli, G. A., 1999, Reconstruction of brain networks by algorithmic amplification of morphometry data, *Lect. Notes Comp. Sci.* **1606**:25–33.
- Shetty, A. K., and Turner, D. A., 1999, Aging impairs axonal sprouting response of dentate granule cells following target loss and partial deafferentation, *J. Comp. Neurol.* **414**(2):238–254.
- Stepanyants, A., Tamas, G., and Chklovskii, D. B., 2004, Class-specific features of neuronal wiring, *Neuron.* **43**(2):251–259.

- Tamamaki, N., Abe, K., and Nojyo, Y., 1988, Three-dimensional analysis of the whole axonal arbors originating from single CA2 pyramidal neurons in the rat hippocampus with the aid of a computer graphic technique, *Brain Res.* **452**(1–2):255–272.
- Turner, D. A., Cannon, R. C., and Ascoli, G. A., 2002, Web-based neuronal archives: neuronal morphometric and electrotonic analysis, In: Kotter, R. (ed.), *Neuroscience Databases—A Practical Guide*, Amsterdam: Elsevier, pp. 81–98.
- Van Ooyen, A., Duijnhouwer, J., Remme, M. W. H., and Van Pelt, J., 2002, The effect of dendritic topology on firing patterns in model neurons, *Network* **13**:311–325.
- Van Ooyen, A., and Van Pelt, J., 2002, Competition in neuronal morphogenesis and the development of nerve connections, In: Ascoli, G. A. (ed.), *Computational Neuroanatomy: Principles and Methods*, Totowa, NJ: Humana Press, pp. 219–244.
- Vetter, P., Roth, A., and Hausser, M., 2001, Propagation of action potentials in dendrites depends on dendritic morphology, *J. Neurophysiol.* **85**(2):926–937.
- Winslow, J. L., Jou, S. F., Wang, S., and Wojtowicz, J. M., 1999, Signals in stochastically generated neurons, *J. Comput. Neurosci.* **6**(1):5–26.
- Wolf, E., Birinyi, A., and Pomahazi, S., 1995, A fast three-dimensional neuronal tree reconstruction system that uses cubic polynomials to estimate dendritic curvature, *J. Neurosci. Methods* **63**:137–145.
- Yates, P. A., Holub, A. D., McLaughlin, T., Sejnowski, T. J., and O’Leary, D. D., 2004, Computational modeling of retinotopic map development to define contributions of EphA-ephrinA gradients, axon–axon interactions, and patterned activity, *J. Neurobiol.* **59**(1):95–113.
- Young, M. P., and Scannell, J. W., 1996, Component-placement optimization in the brain, *Trends Neurosci.* **19**(10):413–415.
- Zaborszky, L., Csordas, A., Buhl, D., Duque, A., Somogyi, J., and Nadasdy, Z., 2002, Computational anatomical analysis of the basal forebrain corticopetal system, In: Ascoli, G. A. (ed.), *Computational Neuroanatomy: Principles and Methods*, Totowa, NJ: Humana Press, pp. 171–198.